



## Experimental Study on Separated Low Yield Point Steel Plate Wall with Slits

Jie Tian<sup>(1)</sup>, Wei Huang<sup>(2)</sup>, Xiuzhen Pan<sup>(3)</sup>

<sup>(1)</sup> Professor, School of Civil & Architecture Engineering, Xi'an University of Technology, Xi'an, China, tianjie@xaut.edu.cn

<sup>(2)</sup> Professor, School of Civil Engineering, Xi'an University of Architecture & Technology, Xi'an, China, qqhuangwei2005@126.com

<sup>(3)</sup> Associate Professor, School of Civil & Architecture Engineering, Xi'an University of Technology, Xi'an, China, panxiuzhen@163.com

### Abstract

A new type of earthquake-resisting element, composing of steel frame lattice and embedded low yield point steel plate with slits, is proposed. In this system, the steel frame lattice is composed of small ribbed beams and ribbed columns, and the embedded steel plate is scattered in several small frame lattice. Since steel plate is separated into smaller sizes, it is easy to meet the requirements of the steel plate to prevent buckling. Being different from the reinforced rib of the conventional stiffened steel plate shear wall, the ribbed beam and the ribbed column of the new steel plate walls are the main load-bearing components, which can effectively improve the lateral stiffness and bearing capacity of the low yield point steel plate with slits, and can also provide a certain vertical bearing capacity. The stiffness, bearing capacity and vibration characteristics of the steel plate walls can be adjusted by changing the configuration of the steel frame lattice as well as the vertical slits of the embedded steel plate. Because of its unique structural composition, it is easy to replace and repair after earthquake.

In this paper, test results are presented for eight steel plate wall specimens of roughly 1/2 scale, which were subjected to static monotonic and cyclic lateral loading. The embedded steel plate used the low yield point steel LYP100 and the steel frame lattice used ordinary low carbon steel Q235B. These tests provide data on general behavior of the walls, which provides the basis for models to calculate the strength and stiffness of the steel plate wall. The experimental results show that the new steel plate wall has reasonable energy dissipation mechanism, failure mode and good hysteretic performance. The existence of frame lattice effectively prevented or delayed the out-of-plane buckling of the embedded steel plate, and greatly improved the lateral stiffness and bearing capacity of the specimen. There was no obvious degradation of strength and stiffness of the specimens under large storey drift angle. Due to the ductile bending deformation produced by a series of strips of the steel plate, coupled with the existence of frame lattice, the steel plate wall has good ductility, the storey drift angle of the vertex can reach more than 5%, and the ductility coefficient can reach more than 8. The function of frame lattice made the embedded low yield point steel plate energy dissipation sufficient, and greatly improved the energy dissipation capacity of steel plate wall. The separated low yield point steel plate wall with slits is a kind of resistance to lateral forces and energy dissipation elements with excellent seismic performance.

*Keywords: separated; low yield point steel; steel plate wall with slits; test; seismic behavior*



## 1. Introduction

A steel plate shear wall with slits was proposed by Hitaka et al.(2003,2007) (see fig.1)[1-2].The basic concept of these walls is for the steel plate segments between the slits to behave as a series of flexural links,which undergo large flexural deformations relative to their shear deformations,to provide a fairly ductile response without the need for heavy stiffening of the wall.In this system,these walls are earthquake-resisting elements that are connected to moment frames by high-strength tension friction bolts.Strength and stiffness can be adjusted independently by changing the slit configuration such as interval,length and number of layers of slits.The wall is need not occupy the full beam span,thus accommodating door or window opening adjacent to the wall.Three buildings incorporating steel plate shear wall with slits have been constructed in Japan.However, the stiffness and bearing capacity of the wall are weakened by the slits.As in the two applications,the steel plate shear wall is designed to carry approximately 10% to 25% of the seismic base shear, with the balance being carried by the moment frames.

Energy dissipation devices or dampers made of low yield point steel can significantly reduce structural damage under major earthquakes, and can avoid or reduce post-earthquake repair work, which has attracted more and more attention in engineering, especially in Japan[3-6].The results were published at the World Earthquake Engineering Conferences(WCEE)[7-11]. In recent years, China have also carried out research in this area[10-13]. However, the prominent problem of the steel plate shear wall is the out-of-plane buckling of the embedded steel plate, while the steel plate shear wall with slits is even more susceptible to out-of-plane buckling than conventional steel shear walls,because the steel panel is not welded to its adjacent columns,as is the care for conventional walls.When the low yield point steel plate is used as resistance to lateral forces element, especially steel plate with slits, it cannot provide enough lateral stiffness and bearing capacity for the structure. in addition, the existing steel plate shear walls only consider to bear the shear force transmitted along the frame beam or column, but ignore the vertical load that may occur in the structure.

Based on the study of the above steel plate shear wall, the author proposes a new type of separated low yield point steel plate wall with slits[14],which is composed of steel frame lattice and embedded low yield point steel plate with slits(see fig.2).The steel frame lattice is composed of small ribbed beams and ribbed columns, and the embedded steel plate is scattered in several small steel lattices.Because of the small size of the steel plate, it is easy to meet the requirements of the steel plate to prevent buckling. Being different from the reinforced rib of the conventional stiffened steel plate shear wall, the ribbed beam and the ribbed column of the new steel plate walls are the main load-bearing components, and the function of the steel frame lattice effectively improves the lateral stiffness and horizontal bearing capacity of the steel plate wall, and can provide a certain vertical bearing capacity.The stiffness,bearing capacity and vibration characteristics of the walls can be adjusted by changing the configuration of the steel frame lattice.The objectives and scope of this paper is to verify the seismic performance of this new earthquake-resisting element through the quasi-static test.

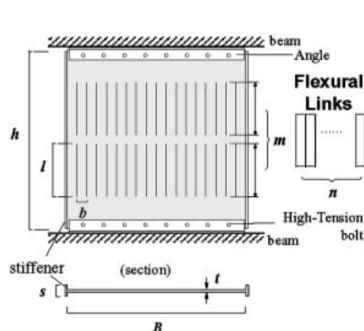


Fig.1 Steel plate wall with slits<sup>[1,2]</sup>

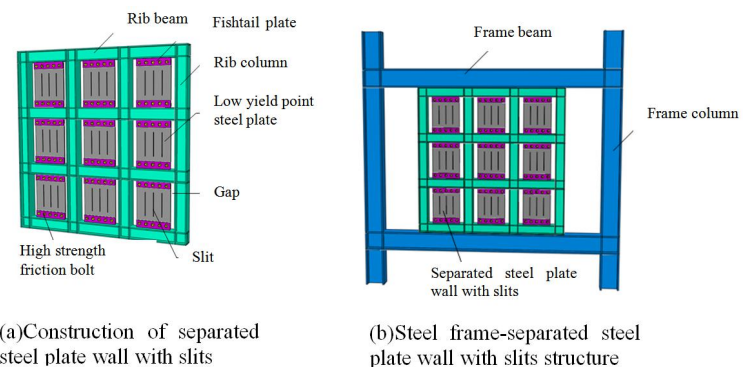


Fig.2 Separated low yield point steel plate wall with slits system



## 2. Test programme

### 2.1 Specimen

There are 8 specimens MSW-1~MSW-8 in this test, roughly 1/2 scale. The MSW-1 is a two-beam two-column type, MSW-2 is a three-beam three-column type, MSW-3~MSW-6 are a four-beam four-column type, MSW-7 is a four-beam three-column type, and MSW-8 is a three-beam four-column type. The connection of the ribbed beam with the ribbed column, except that the MSW-6 was bolted, the other specimens were welded. The embedded steel plate was only connected with the ribbed beam through the fishtail plate, while there was a gap of 50mm between the steel plate and the ribbed column. In addition to MSW-4 using welding, the embedded steel plate was bolted to the fishtail plate. The embedded steel plate used the low yield point steel LYP100 produced by China Angang with the yield strength of 114MPa and the plate thickness of 10mm. The steel used for the frame lattice was the H-section steel of Q235B, a steel commonly used in China, except for the top beam with HN200×100×5.5×8, the other ribbed beams and rib columns were all used with HW100×100×6×8. The bolts used high strength friction bolts of grade 10.9. The width of the slits of the embedded steel plate was 5mm, and the other analysis parameters are shown in Table 1 and Fig.1.

Table 1 Specimens

Specimen	Feature	Height× Width /mm	h×B×t/mm	h/B	B/t	b/t	l/mm	Loading
MSW -1		1700×1600	1400×1300×10	1.08	130	10.8	350	Cyclic
MSW -2		1700×1600	650×550×10	1.18	55	9.2	290	Cyclic
MSW -3		1700×1600	400×300×10	1.33	30	7.5	200	Cyclic
MSW -4		1700×1600	400×300×10	1.33	30	7.5	200	Cyclic
MSW -5		1700×1600	400×300×10	1.33	30	7.5	200	Mono
MSW -6		1700×1600	400×300×10	1.33	30	7.5	200	Cyclic Mono
MSW -7		1700×1600	400×550×10	0.73	55	7.9	200	Cyclic Mono
MSW -8		1700×1600	650×300×10	2.17	30	7.5	290	Cyclic

### 2.2 Test set-up

The horizontal loading device adopted an electro-hydraulic servo program control system. One end of the MTS actuator was connected to the loading end at the top beam of the specimen, and the other end was fixed on the reaction force wall. The horizontal load was applied to the specimen by the 1000kN actuator. The vertical axial force was provided by the 1000kN synchronous hydraulic jack, and the roller device was set between the Jack and the distribution beam, so that the jack can keep the real-time horizontal movement with



the column top. Lateral support was provided for the specimen at the center elevation of the top beam to prevent the out-of-plane instability of the specimen. Test set-up is shown in Figure 3~10.

### 3. Test results and discussion

#### 3.1 Failure process

##### 3.1.1 Specimen MSW-1

Firstly, the vertical load was applied to the top of the ribbed column with the axial compression ratio of 0.1. Secondly, the horizontal load was applied according to each stage 40kN, and each stage load was cycled once. When loaded to 240kN, the embedded steel plate yielded, the column foot of the ribbed column yielded, and the load displacement curve of the tracking record began to be nonlinear, which was determined that the deformation of the steel plate wall had entered the elastic-plastic stage, at this time, the displacement of the specimen was defined as the yield displacement of  $\delta_y=12\text{mm}$ . Subsequently, the loading was controlled by a multiple of the yield displacement, three cycles per stage. When loaded to 24mm, the embedded steel plate produced slight shear and bending deformation; when loaded to 36mm, the steel plate had obvious bending deformation, and the out-of-plane buckling appeared, and the strips of steel plate bulged out of the plane in a basin shape; when loaded to 48mm, the steel plate has appeared large out-of-plane buckling, and the basin-like deformation has been further developed, at this time, the specimen has reached the maximum ultimate bearing capacity of 275kN. With the further increase of the load, when loaded to 60mm, the external buckling of the steel plate was serious, but the whole frame lattice of the specimen remained deformed in the plane; when loaded to 72mm, the basin-like deformation of the steel plate continued to develop, and a certain buckling occurred at the flange of the rib column; when loaded to 80mm, the steel plate basin-like deformation was further developed, and the buckling of the flange of the rib column foot was further increased; when loaded to 96mm, the steel plate basin-like deformation was larger, and the rib column foot formed a plastic hinge, it was considered that the specimen has reached the failure loading and the test stopped, and the top storey draft angle of the specimen has reached 6.0%, the ductility coefficient was  $\delta / \delta_y=8$ . The failure state of the specimen MSW-1 is shown in fig.3.



Fig.3 Failure state of specimen MSW-1

##### 3.1.2 Specimen MSW-2

Firstly, the vertical load was applied to the top of the ribbed column with the axial compression ratio of 0.07. Secondly, the horizontal load was applied according to each stage 20kN, one cycle per stage. When loaded to



300kN, the embedded steel plate yielded entirely, the end of ribbed beam and the bottom of ribbed column yielded, and the load displacement curve of the tracking record began to be nonlinear, at which time the displacement of the specimen was defined as the yield displacement being  $\delta_y = 12\text{mm}$ . Subsequently, the loading was controlled by a multiple of the yield displacement, three cycles per stage. When loaded to 24mm, the embedded steel plate had slight shear and bending deformation; when loaded to 36mm, the steel plate had obvious shear and bending deformation; when loaded to 48mm, steel plate presented a series of bending deformation of the strips and a certain out-of-plane deformation occurred, at which time the specimen has reached the maximum ultimate bearing capacity of about 450kN. When loaded to 60mm, the out-of-plane deformation of the steel plate was further increased, and the edge rib column had a certain bending deformation; when loaded to 72mm, the out-of-plane deformation of the steel plate was more severe and bulged out of the plane, showing a basin shape. A crack appeared at the weld seam of the middle rib beam and the edge rib column, and the tear gradually occurred during the subsequent loading process. When loaded to 84mm, the basin-like deformation of the steel plate further developed and the vertical slits opened; when loaded to 96mm, the shear failure occurred at the weld of the middle rib beam and the side rib column, and the plastic angle appeared at the foot and the top of the rib column, it was considered that the specimen has reached the failure load and stopped the test, and the top storey draft angle of the specimen has reached 6.0%, the ductility coefficient was  $\delta / \delta_y = 8$ . The failure state of the specimen MSW-2 is shown in fig.4.

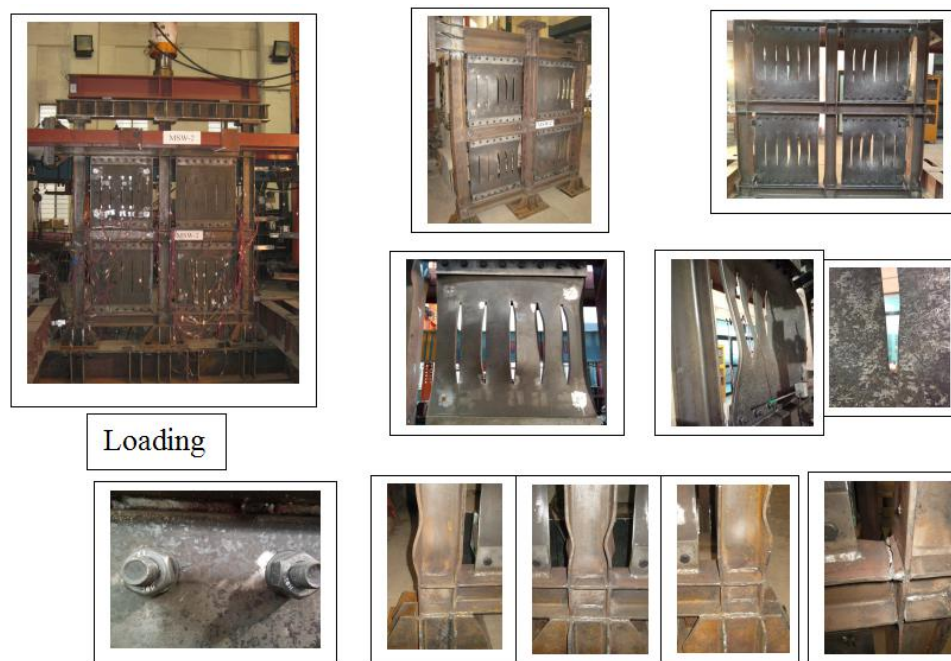


Fig.4 Failure state of specimen MSW-2

### 3.1.3 Specimen MSW-3

Firstly, the vertical load was applied to the top of the ribbed column with the axial compression ratio of 0.05. Secondly, the horizontal load was applied according to each stage 80kN, one cycle per stage. When loaded to 400kN, the embedded steel plate yielded, the end of the bottom ribbed beam and the foot of the bottom ribbed column yielded, and the load displacement curve of the tracking record began to be nonlinear, at which time the displacement of the specimen was defined as the yield displacement, being of  $\delta_y = 12\text{mm}$ . Subsequently, the loading was controlled by a multiple of the yield displacement, three cycles per stage. When loaded to 24mm, the embedded steel plate has no obvious deformation; when loaded to 36mm, the steel plate produced a slight shear deformation; when loaded to 48mm, the steel plate in the bottom frame lattice presented a certain bending deformation, and there was no obvious out-of-plane buckling; when loaded to 60mm, the



steel plate of the bottom frame lattice showed obvious bending deformation, the embedded steel plate of the upper frame lattice had obvious shear deformation, and the slip phenomenon appeared between the embedded steel plate and the bolt. When loaded to 72mm, the steel plate of the bottom frame lattice showed a certain out-of-plane buckling, but the steel plate of the upper frame lattice had no out-of-plane buckling, the flange of the middle rib beam as well as the flange of the rib column foot had certain buckling deformation; when loaded to 84mm, the strip of the steel plate of the bottom frame lattice bulged out of the plane and was basin-like, while the steel plate of the upper frame lattice had only slight out-of-plane buckling; at this time the specimen reached the maximum ultimate bearing capacity of about 670kN. When loaded to 96 mm, the basin-like deformation of the steel plate in the bottom frame lattice was further developed, while the steel plate in the upper frame lattice had only a certain out-of-plane buckling, the column foot of the bottom ribbed column formed a plastic hinge, and the overall frame of the specimen remained as in-plane deformation without buckling instability. When loaded to 108mm, the bottom frame lattice of the specimen was deformed seriously, and the flange of the column foot of the edge ribbed column appeared to tear as pulling direction, it was considered that the specimen has reached the failure load, and the test was stopped, and the top storey draft angle of the specimen reached 6.75%, the ductility coefficient was  $\delta / \delta_y = 9$ . The failure state of the specimen MSW-3 is shown in fig.5.



Fig.5 Failure state of specimen MSW-3

### 3.1.4 Specimen MSW-4

Firstly, the vertical load was applied to the top of the ribbed column with the axial compression ratio of 0.05. Secondly, the horizontal load was applied according to each stage 80kN, one cycle per stage. When loaded to 400kN, the embedded steel plate yielded, the end of the bottom ribbed beam and the foot of the bottom ribbed column yielded, and the load displacement curve of the tracking record began to be nonlinear, at which time the displacement of the specimen was defined as the yield displacement, being of  $\delta_y = 10$ mm. Subsequently, the loading was controlled by a multiple of the yield displacement, three cycles per stage. When loaded to 20mm, the embedded steel plate had no obvious deformation; when loaded to 30mm, the steel plate presented a certain shear and bending deformation; when loaded to 40mm, the band bending deformation of the steel plate of the bottom frame lattice increased, but the steel plate in the second and third frame layers was still dominated by shear deformation; when loaded to 50mm, the strip of the steel plate inside the bottom frame lattice presented large bending deformation and obvious out-of-plane buckling, while the



steel plate of the upper frame lattice did not see obvious out-of-plane buckling, at this time, the specimen reached the maximum ultimate bearing capacity of about 680kN; when loaded to 60mm, the bending deformation and out-of-plane buckling of the steel plate strip in the bottom frame lattice were further increased; when loaded to 70 mm, the steel plate in the upper frame lattice also produced a certain bending deformation and out-of-plane buckling, and plastic buckling deformation appeared at the flange of the upper and lower ends of the bottom ribbed column; when loaded to 80mm, the bottom frame lattice embedded steel plate appeared a large basin-like out-of-plane buckling, and the flange and web at the upper and lower ends of the bottom frame lattice ribbed column were torn, to prevent the specimen from collapsing and protect the instrument, the loading was stopped, and the top storey draft angle was 5%, the ductility coefficient was  $\delta / \delta_y = 8$ . The failure state of the specimen MSW-4 is shown in fig.6.



Fig.6 Failure state of specimen MSW-4

### 3.1.5 Specimen MSW-5

Firstly, the vertical load was applied to the top of the ribbed column with the axial compression ratio of 0.05. Secondly, the horizontal single-pull load was applied according to each stage 80kN, and each stage load was applied once. When loaded to 400kN, the embedded steel plate yielded, the end of the bottom ribbed beam and the foot of the bottom ribbed column yielded, and the load displacement curve of the tracking record began to be nonlinear, at which time the displacement of the specimen was defined as the yield displacement, being of  $\delta_y = 12\text{mm}$ . Subsequently, the single-pull loading was controlled by a multiple of the yield displacement, one time per stage. With the increasing of horizontal single-pull loading, the embedded steel plate was gradually transformed from shear deformation to bending deformation of strips, and the bolts appeared a certain slip phenomenon. When pulled to 240mm, limited by the equipment, stopped the test. In the end, the top storey draft angle of the specimen reached 15.0%, the ductility coefficient was  $\delta / \delta_y = 20$ , while the ultimate bearing capacity reached 734kN, and the whole frame of the specimen was still maintained in the plane deformation without instability, showing good ductility. The failure state of the specimen MSW-5 is shown in fig.7.



Fig.7 Failure state of specimen MSW-5

### 3.1.6 Specimen MSW-6

Firstly, a vertical load with an axial compression ratio of 0.05 was applied to the top of the ribbed column. Secondly, the horizontal load was applied at each stage of 80kN, one cycle per stage. When loaded to 400kN, the embedded steel plate yielded, the end of the bottom ribbed beam and the foot of the bottom ribbed column yielded, and the load displacement curve of the tracking record began to be nonlinear, at which time the displacement of the specimen was defined as the yield displacement, being of  $\delta_y = 15\text{mm}$ . Subsequently, the loading was controlled by a multiple of the yield displacement. When cyclic loading to 30mm, the embedded steel plate had no obvious deformation; when cyclic loading to 45mm, the steel plate produced a slight shear deformation. When cyclic loading to 60mm, the steel plate had obvious shear and bending deformation; when cyclic loading to 75mm, the bending deformation of the steel plate was further increased, and after one cycle of the 75mm, the angle steel at the connection between the rib beam and the rib column was broken and then changed to single-push loading. When pushed to 120mm, the embedded steel plate presented the larger bending deformation of the strips, the column foot of the bottom ribbed column formed the plastic hinge, and the test stopped. Finally, the ultimate bearing capacity of the specimen was 585kN, and the top storey draft angle of the specimen reached 7.5%, the ductility coefficient was  $\delta / \delta_y = 8$ . During the whole loading process, the bolt did not appear obvious slip, and the fishtail plate and bolt were basically intact. Except for one bolt connection fracture failure, the other bolts connection between the ribbed beam and the ribbed column were well, and the deformation coordination performance between the embedded steel plate and the frame lattice was good. The failure state of the specimen MSW-6 is shown in fig.8.





Fig.8 Failure state of specimen MSW-6

### 3.1.7 Specimen MSW-7

Firstly, a vertical load with an axial compression ratio of 0.07 was applied to the top of the ribbed column. Secondly, the horizontal load was applied according to each stage 80kN, one cycle per stage. When loaded to 400kN, the embedded steel plate yielded, the end of the bottom ribbed beam and the foot of the bottom ribbed column yielded, at which time the displacement of the specimen was defined as the yield displacement, being of  $\delta_y = 10\text{mm}$ . Subsequently, the loading was controlled by a multiple of the yield displacement. When cyclic loading to 20mm, the embedded steel plate had no obvious deformation; when cyclic loading to 20mm, the steel plate inside the bottom frame lattice produced a slight shear deformation; when cyclic loading to 30mm, the bottom steel plate had obvious shear deformation; when cyclic loading to 40 mm, the bottom steel plate showed a certain bending deformation; when cyclic loading to 50mm, as the positive direction (push direction) was loaded, the web of the top beam underwent local buckling instability, and then loading was changed to a single pull. When pulled to 112mm, the bottom frame lattice was seriously deformed, the bottom steel plate strip presented a large bending deformation, and the column foot produced plastic buckling deformation, which was considered that the specimen was destroyed and the test was stopped. In the end, the ultimate bearing capacity of the specimen was about 670kN, the top storey draft angle of the specimen reached 7.0%, the ductility coefficient was  $\delta / \delta_y = 11$ , and the steel plate wall did not appear obvious out-of-plane buckling. The failure state of the specimen MSW-7 is shown in fig.9.

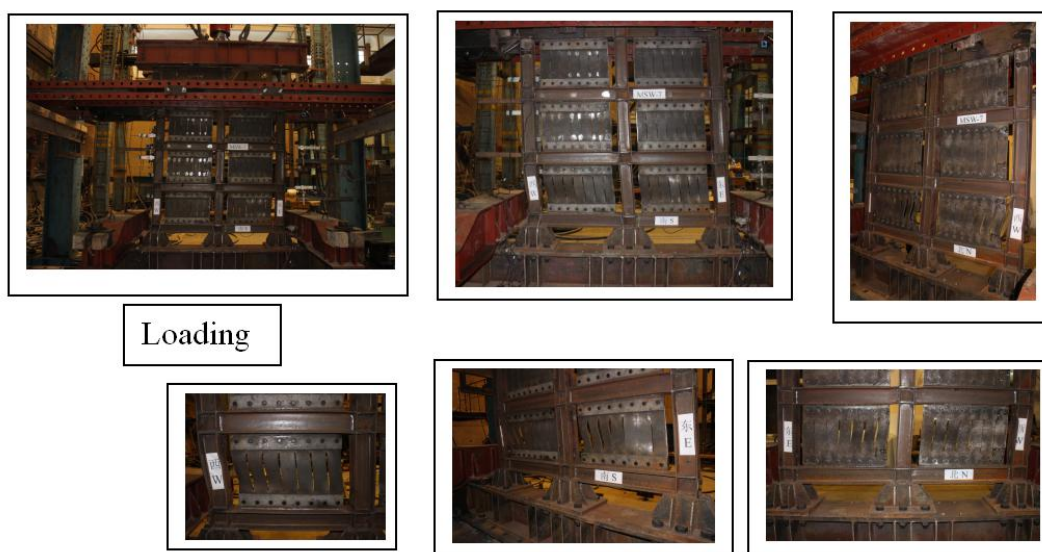


Fig.9 Failure state of specimen MSW-7



### 3.1.8 Specimen MSW-8

Firstly, the vertical load with the axial compression ratio of 0.05 was applied to the top of the ribbed column. Secondly, the horizontal load was applied according to each stage 80kN, one cycle per stage. When loaded to 320kN, the embedded steel plate yielded, the end of the bottom ribbed beam and the foot of the bottom ribbed column yielded, and the load displacement curve of the tracking record began to be nonlinear, at which time the displacement of the specimen was defined as the yield displacement, being of  $\delta_y = 15\text{mm}$ . Subsequently, the loading was controlled by a multiple of the yield displacement, three cycles per stage. When loaded to 30mm, the embedded steel plate has no obvious deformation; when loaded to 45mm, the steel plate had obvious shear and bending deformation; when loaded to 60mm, the strip of the steel plate presented a large bending deformation, and the specimen has reached the ultimate bearing capacity of 493kN; when loaded to 75mm, the bending deformation of the steel plate was further developed; when loaded to 90mm, the steel plate showed a certain out-of-plane buckling; when loaded to 105mm, there was a large plastic deformation at the column foot of the rib column, and the fracture failure occurred at the weld between the middle rib beam and the edge rib column, but the whole frame of the specimen was still maintained in the plane; when loaded to 120mm, the column foot of the ribbed column formed a plastic angle, and the bending deformation of the steel plate strips developed fully, and there were certain out-of-plane buckling of the steel plate. At this time, the top storey draft angle of the specimen reached 7.5%, the ductility coefficient was  $\delta / \delta_y = 8$ , which is considered that the specimen had reached the failure load and stopped the test. The failure state of the specimen MSW-8 is shown in Fig. 10.



Fig.10 Failure state of specimen MSW-8

As above, the failure order of each specimen, first was the embedded steel plate, then was the rib beam, the rib column, the last was the column foot of the rib column to form the plastic angle, which could be graded to destroy, graded to release energy, showing a reasonable energy dissipation mechanism and failure mode. During the whole loading process, the deformation coordination performance between the embedded steel plate and the frame lattice was good. The function of frame lattice effectively prevented or delayed the out-of-plane buckling of the embedded low yield point steel plate, and greatly improved the ultimate bearing capacity of steel plate wall. Despite the local out-of-plane buckling of the steel plate during the large displacement control loading, the overall frame of the specimen has always been kept deformed in the plane, and there was no obvious degradation of strength and stiffness of the specimen as well as sudden collapse phenomenon, showing



good stability. Since shear steel plate was transformed into a series of bending strips due to the slits, providing a large ductility, coupled with the steel frame lattice, the plate steel wall has good ductility, which the top storey draft angle of the specimen has reached more than 5%, and the ductility coefficient has reached more than 8.

### 3.2 Hysteretic performance

Figure 11 shows that the shape of the hysteresis curve of specimens is full, indicating that the separated low yield point steel plate wall with slits has a strong energy dissipation capacity. For the specimens MSW-1, MSW-2, MSW-3, MSW-6, MSW-7 and MSW-8, the connection of the embedded steel plate with the ribbed beam was bolted, during the control loading process, the bolt would slip somewhat, resulting in a certain pinch slip phenomenon in the hysteresis curve. However, with the increasing of the number of ribbed beams and ribbed columns, the pinch slip phenomenon of the specimen was reduced. Since the embedded steel plate in the specimen MSW-4 was welded with the fishtail plate, there was no slip, which the hysteresis curve was more full. The load-displacement skeleton curves of specimens are shown in figure 12, the existence of the frame lattice, and the increasing in the number of ribbed beams and ribbed columns, which greatly improved the initial stiffness and ultimate bearing capacity of the specimens. Figure 13 is the energy dissipation value of the specimens, the frame lattice effectively prevented or delayed the out-of-plane buckling of the embedded steel plate, which made the embedded low yield point steel plate energy dissipation sufficient, and greatly improved the energy dissipation capacity of the steel plate wall.

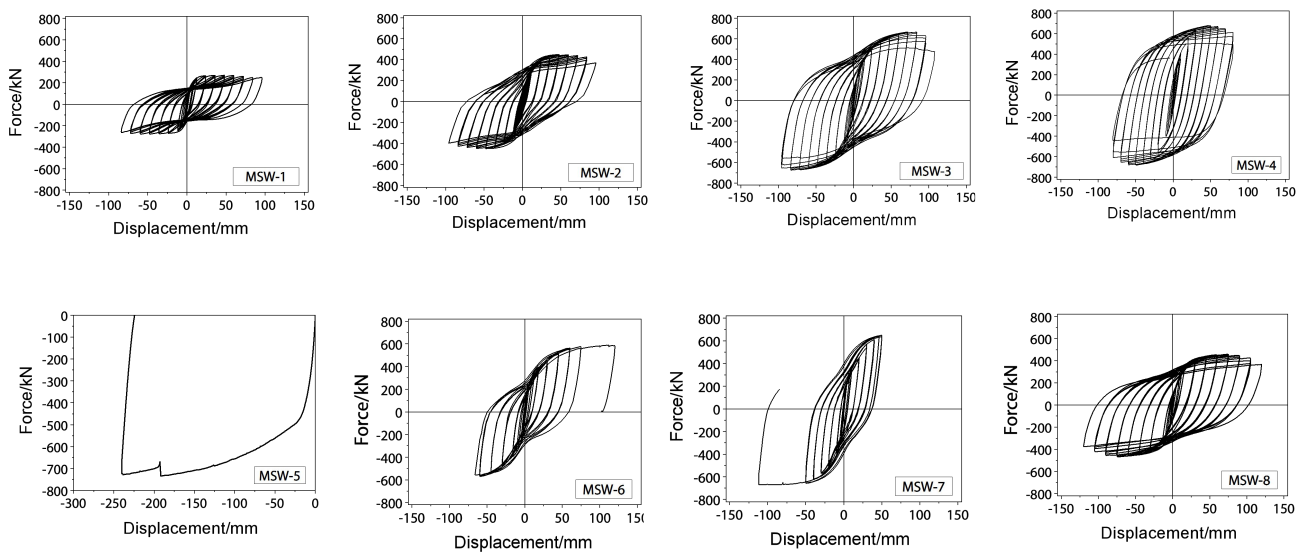


Fig.11 Hysteresis curves of specimens

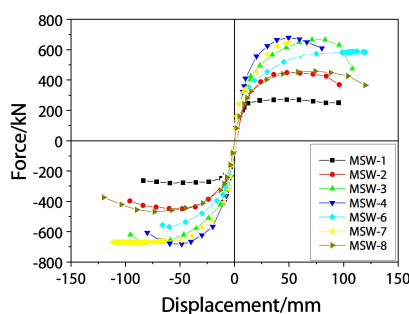


Fig.12 Keleton curves of specimens

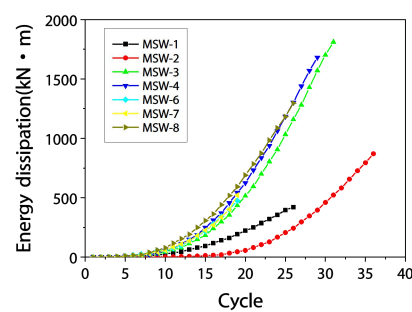


Fig.13 Energy dissipation of specimens



#### 4. Summary and conclusion

A new type of separated low yield point steel plate wall with slits was presented. The seismic behavior of the new steel plate wall was investigated by the quasi-static test of eight specimens. The experimental results showed that the new steel plate wall had reasonable energy dissipation mechanism, failure mode and good hysteretic performance. The existence of frame lattice effectively prevented or delayed the out-of-plane buckling of the embedded steel plate, and greatly improved the lateral stiffness and bearing capacity of the specimen. Under the large displacement controlled loading, the specimen showed no obvious degradation of strength and stiffness as well as sudden collapse, showing good stability. Due to the ductile bending deformation produced by a series of strips of the steel plate, coupled with frame lattice, the new steel plate wall has good ductility, which top storey draft angle of the specimen can reach more than 5%, and the ductility coefficient can reach more than 8. The function of frame lattice made the embedded low yield point steel plate energy dissipation sufficient, and greatly improved the energy dissipation capacity of steel plate wall. The separated low yield point steel plate wall with slits is a kind of resistance to lateral forces and energy dissipation elements with excellent seismic performance.

#### 5. Acknowledgements

Current research has been financially supported by the National Natural Science Foundation of China Research Project (No.51078310) .

#### 6. References

- [1] Toko Hitaka, Chiaki Matsui (2003): Experimental study on steel shear wall with slits. *Journal of Structural Engineering*, **129** (5), 586-595.
- [2] Toko Hitaka, Chiaki Matsui, Junichi Sakai (2007): Cyclic Test on Steel and Concrete-filled Tube Frames with Slit Walls. *Earthquake Engineering & Structural Dynamics*, **36**, 707-727.
- [3] Nakashima M, Iwai S, Iwata M, Takeuchi T, Konomi S, Akazawa T, Saburi K. O. Energy dissipation behavior of shear panels made of low yield steel. *Earthquake Engineering & Structural Dynamics*, 1994, **23**:1299-1313
- [4] Kihara K, Kitamura H, Torii S (1997): Design of Response Control Walls Using Low Yield Strength Steel. *Journal of Constructional Steel*, **5**, 577-588.
- [5] Kamura H, Katayama T, Ito S, Hirota M, Ito S, Wada A, Uchikoshi M (1997): Study on shear wall with Low Yield Strength Steel for Hysteretic damper. *Steel Construction Engineering*, **5** (20), 9-16.
- [6] Connor J, Wada A, Iwata M, Huang Y (1997): Damage-controlled Structures. I: Preliminary Design Methodology for seismically active regions. *Journal of Structural Engineering*, **123**, 423-431.
- [7] Kiyoshi TANAKA and Yasuhito SASAKI (2000): Hysteretic performance of shear panel dampers of ultra low yield strength steel for seismic response control of building. *12<sup>th</sup> World Conference on Earthquake Engineering*, Auckland, New Zealand.
- [8] Yoshihiro OHTA, Hirofumi KANEKO, Masahito KIBAYASHI, Masayuki YAMAMOTO, Tetuya MUROYA, Kazutomi NAKANE (2004): Study on shear panel dampers using low yield strength steel applied to reinforced concrete buildings. *13<sup>th</sup> World Conference on Earthquake Engineering*, Vancouver, Canada.
- [9] H.B. Ge, K. Kaneko and T. Usami (2008): Capacity of stiffened steel shear panels as a structural control damper. *14<sup>th</sup> World Conference on Earthquake Engineering*, Beijing, China.
- [10] Ning Ma, Jinping Ou, Hui Li (2012): Experimental Study of Low-yield Strength Steel Buckling Restrained Brace. *15<sup>th</sup> World Conference on Earthquake Engineering*, Lisbon, Portugal.
- [11] Jie TIAN, Zhichao Yan, Junfa ZHANG, Yunher LIU (2017): A multi-ribbed composite wall with low-yield strength steel for seismic mitigation. *16<sup>th</sup> World Conference on Earthquake Engineering*, Santiago, Chile.
- [12] Keh-Chyuan Tsai, Chao-Hsien Li, Chih-Han Lin, Ching-Yi Tsai and Yi-Jer Yu (2010): Cyclic tests of four two-story narrow steel plate shear walls. Part 1: Analytical studies and specimen design. *Earthquake Engineering and Structural Dynamics*, 2010, **39**:775-799
- [13] Chao-Hsien Li, Keh-Chyuan Tsai, Chih-Han Lin and Pei-Ching Chen (2010): Cyclic tests of four two-story narrow steel plate shear walls. Part 2: Experimental results and design implications. *Earthquake Engineering and Structural Dynamics*, 2010, **39**:801-826
- [14] TIAN Jie, YAN Zhichao (2015): Separated steel plate shear wall. Patent ZL201210346753.9, PRC.